First observation of isomeric states in math xmlns="http://www.w3.org/1998/Math/MathML">mmultiscripts>mi>Zr/mi>mprescripts>/mprescripts>none>/none>mn>111/mn>/mmultiscripts>mo>,/mo>mo> /mo>mmultiscripts>mi>Nb/mi>mprescripts>/mprescripts>none>/none>mn>113/mn>/mmultiscripts>/math>, and math xmlns="http://www.w3.org/1998/Math/MathML">mmultiscripts>mi>Mo/mi>mprescripts>/mprescripts>none>/none>mn>115/mn>/mmultiscripts>/math>

J. Wu et al.

Phys. Rev. C **106**, 064328 — Published 26 December 2022

DOI: 10.1103/PhysRevC.106.064328

First observation of isomeric states in ^{111}Zr, ^{113}Nb and ^{115}Mo

J. Wu,[1] S. Nishimura,[2] P.-A. Söderström,[3] A. Algora,[4,5] J.J. Liu,[2,6] V.H. Phong,[2] Y.Q. Wu,[7] F.R. Xu,[7] J. Agramunt,[4] D.S. Ahn,[2] T.A. Berry,[8] C.G. Bruno,[9] J.J. Bundgaard,[10] R. Caballero-Folch,[11] A.C. Dai,[7] T. Davinson,[9] I. Dillmann,[11] A. Estrade,[12] A. Fijakowska,[13,14] N. Fukuda,[2] S. Go,[2] R.K. Grzywacz,[10,15] T. Isobe,[2] S. Kubono,[2] G. Lorusso,[2,8,16] K. Matsui,[2,17] A.I. Morales,[4] N. Nepal,[12] S.E. Orrigo,[4] B.C. Rasco,[15] K.P. Rykaczewski,[15] H. Sakurai,[2] Y. Shimizu,[2] D.W. Stracener,[15] T. Sumikama,[2] H. Suzuki,[2] J.L. Tain,[4] H. Takeda,[2] A. Tarifeño-Saldivia,[4,18] A. Tolosa-Delgado,[4] M. Wolińska-Cichocka,[19] and R. Yokoyama[10]

[1] *National Nuclear Data Center, Brookhaven National Laboratory, Upton, NY 11973, USA*
[2] *RIKEN Nishina Center, 2-1 Hirosawa, Wako-shi, 351-0198, Saitama, Japan*
[3] *Extreme Light Infrastructure - Nuclear Physics (ELI-NP), Bucharest-Magurele, 077125, Romania*
[4] *Instituto de Fsica Corpuscular (CSIC-Universitat de Valencia), Apartado Correos, 22085, E-46071 Valencia,, Spain*
[5] *Institute of Nuclear Research, ATOMKI, 4026, Debrecen, Hungary*
[6] *Department of Physics, the University of Hong Kong, Pokfulam Road, Hong Kong*
[7] *School of Physics and State Key Laboratory of Nuclear Physics and Technology, Peking University, Beijing, 100871, China*
[8] *Department of Physics, University of Surrey, Guildford, GU2 7XH, United Kingdom*
[9] *School of Physics and Astronomy, University of Edinburgh, Edinburgh, EH9 3FD, United Kingdom*
[10] *Department of Physics and Astronomy, University of Tennessee, Knoxville, 37996, Tennessee, USA*
[11] *TRIUMF, Vancouver, V6T 2A3, British Columbia, Canada*
[12] *Department of Physics and Science of Advanced Materials Program, Central Michigan University,, Mount Pleasant, 48859, Michigan, USA*
[13] *Department of Physics and Astronomy, Rutgers University, New Brunswick, 08854, NJ, USA*
[14] *Faculty of Physics, University of Warsaw, Warsaw, PL-02-093, , Poland*
[15] *Physics Division, Oak Ridge National Laboratory, Oak Ridge, 37830, Tennessee, USA*
[16] *Chemical Medical and Enviromental Science Division, National Physical Laboratory, Teddington TW110LW, United Kingdom*
[17] *Department of Physics, University of Tokyo, Hongo 7-3-1, Bunkyo-ku, 113-0033, Tokyo, Japan*
[18] *INTE-ETSEIB, Universitat Politecnica de Catalunya (UPC), E-08028, Barcelona, Spain*
[19] *Heavy Ion Laboratory, University of Warsaw, Ludwika Pasteura 5A, 02-093, Warszawa, Poland*

(Dated: November 29, 2022)

Isomeric states in the neutron-rich nuclei ^{111}Zr ($T_{1/2}$ = 0.10(7) μs), ^{113}Nb ($T_{1/2}$ = 0.7(4) μs), ^{115}Mo ($T_{1/2}$ = 46(3) μs) were first identified at the Radioactive Ion Beam Factory (RIBF) of RIKEN, by using in-flight fission and fragmentation of a ^{238}U beam at an energy of 345 MeV/u. This is a brief report of the gamma transitions deexciting from isomeric states and half-lives measurements, which provides the first spectroscopy in the nuclear region of protlate-to-oblate shape phase transition around mass A $\approx$ 110.

I. INTRODUCTION

Atomic nuclei consisting of protons and neutrons reflects various kinds of shapes in nature. The existence of "magic numbers" of nucleons at 8, 20, 50, 82 was first pointed out by Dr. M. Goeppert-Mayer and entirely explained after introducing a harmonic oscillator potential with the spin-orbital interaction [1]. The nuclei with doubly "magic" numbers of protons and neutrons exhibits a spherical shape and start deforming when removing or adding protons and neutrons, which is manifest by the occurrence of shape-phase transition driven by the proton-neutron interaction.

The sudden onset of deformation beyond neutron number $N = 60$, first discovered at $_{40}$Zr by Johansson [2], was observed and interpreted with a strong tensor force between proton $\pi g_{9/2}$ and neutron $\nu g_{7/2}$ induced by the increased occupation of the $\nu g_{7/2}$ orbital [3–5]. From thereon, a large degree of connectivity and ground-state quadrupole deformation is manifest toward the middle shell between $N = 50$ and $N = 82$ major closed shells [6, 7]. The maximum deformations of ground state are achieved at $N = 64$ and $N = 62$ for the neutron-rich $_{42}$Mo and $_{40}$Zr isotopes [8, 9], respectively, followed by a well-known region of $Z \approx 40$ and $N \approx 72$ in the nuclear chart with a predicted shape phase transition and shape coexistence between prolate, triaxial, and oblate [10]. The Finite-Range liquid-Drop Model (FRDM) with Bardeen-Cooper-Schrieffer methods indicated the prolate-to-oblate shape phase transition occurs at N = 74, 73, 72 for $_{40}$Zr, $_{41}$Nb, $_{42}$Mo isotopes, respectively [11]. The covariant density functional theory (CDFT) with density-dependent point-coupling parameters, and the Hartree-Fock-Bogoliubov (HFB) calculations with D1S-Gogny interaction, predicted a gradual shape-phase transition from gamma soft rotor at ^{100}Mo ($N = 58$) to well-deformed oblate shape at ^{110}Mo ($N = 68$) [12, 13]. On the experimental side, the ground state of ^{110}Zr was suggested to be a well-deformed shape [14–16], contradicting to a predicted doubly-magic spherical nuclei and the existence of $N = 70$ subshell gap [17].

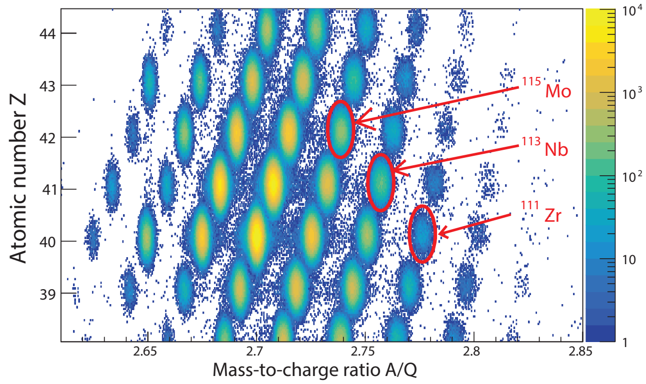

FIG. 1. (color online). Particle identification plot with atomic number (Z) vs mass-to-charge ratio constructed by the TOF-Bρ-ΔE mechanism. The isotopes of ^{111}Zr, ^{113}Nb, ^{115}Mo are tagged with red circles in this plot.

The energy and lifetime measurements of low-lying excited states in $^{100-110}$Zr, did not show any signature of oblate structures in the $_{40}$Zr isotopes [6, 8]. The flat pattern of (ΔE_J-ΔE_{J-1})/E(2_1^+) observed in ^{110}Mo suggests its gamma vibrational feature, inconsistent with the previously suggested gamma-soft rotor [9, 18]. There is no experimental signature of oblate shape and γ-soft rotor observed in the $_{42}$Mo isotopes.

Detailed nuclear structure information in the neutron-rich $A \approx 110$ region has potential implications on the understanding the rapid (r-) neutron capture process [19]. Traditional main r-process nucleosynthesis is not capable of reproducing the observed abundance around the mass $A \approx 110$ region. A new nucleosynthesis mechanism named "weak r-process" is introduced for the compensation [20]. The spectroscopic information in the mass $A \approx 100$ region is extremely rare due to lots of hard-overcome difficulties in the isotope productions. Recent developments of new generation radioactive beam accelerator systems employing the production mechanisms of in-flight fission and fragmentation provide an opportunity to access the first spectroscopic information in this region. Study of the low-lying excited states in the neutron-rich $A \approx 110$ nuclei will serve as a benchmark for testing theoretical calculation, and helps better understand the contributions of main and weak r-process nucleosynthesis.

In the present work, we will briefly report the identification of isomeric states in ^{111}Zr, ^{113}Nb, ^{115}Mo, which will provide a guidance for the future studies with the development of Rare Isotope Facilities.

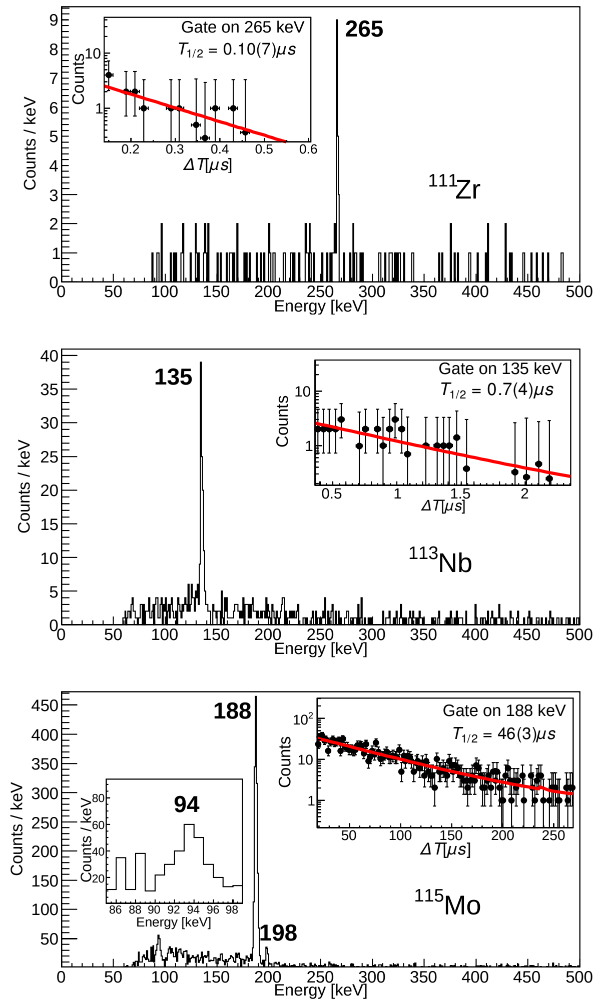

FIG. 2. (color online) Energy spectra of delayed γ rays from ^{111}Zr, ^{113}Nb, ^{115}Mo observed within 0.5 μs, 2.6 μs, 300 μs following implantation, respectively. (Inset) The exponential decay curves from the isomeric decay of ^{111}Zr, ^{113}Nb, ^{115}Mo obtained by gating on the 265-keV, 135-keV, 188-keV transitions, respectively, as well as an energy spectrum of delayed γ rays from ^{115}Mo with a range of 85-99 keV. The half-lives of isomeric states were extracted by fitting the decay curve with the unbinned Maximum Likelihood Method.

II. EXPERIMENT

The neutron-rich isotopes ^{111}Zr, ^{113}Nb, ^{115}Mo were produced by a 345-MeV/u ^{238}U primary beam with an intensity of $\sim$ 30 pnA impinging on a 4-mm ^{9}Be target at the Radioactive Isotope Beam Factory (RIBF). The projectile fission fragments were selected and identified by the large-acceptance BigRIPS and ZeroDegree spectrometers. Separation and identification of the cocktail secondary beam were conducted based on the TOF-Bρ-ΔE principle by employing the radiation detectors along the beam line (see Fig. 1) [21]. The isotopes of interest were finally implanted in the beta counting system

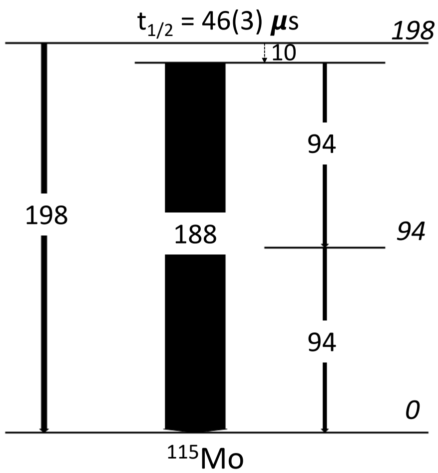

FIG. 3. Partial level scheme of ^{115}Mo obtained in this work. The widths of arrows represent the relative intensities of γ transitions. The dashed arrow shows the unobserved transition due to the small energy of 10-keV.

with a rate of $\sim$ 30 pps, which consists of four Double Sided Silicon Strip Detectors (DSSSDs) and one segmented YSO (Yttrium Orthosilicate, Y_2SiO_5) detector surrounded by 140 proportional counters filled with ^{3}He gas and two HPGe clover-type detectors embedded in a high density polyethylene moderator [22–25]. The emitted prompt and β-delayed γ rays were detected with a full-energy peak γ detection efficiency of 1.93(5)% at 1 MeV calibrated with the ^{133}Ba and ^{152}Eu sources [26–28]. The present work is part of the BRIKEN campaign, which is an international collaborative experimental program aiming to study the β-delayed neutron emission at RIKEN [29].

Data analysis was performed using conventional decay spectroscopy techniques after the identification of implanted ions on an event by event basis [19, 30, 31]. The prompt γ-rays are correlated with the heavy ions by the time-stamp information. The energy spectra of delayed γ rays in ^{111}Zr, ^{113}Nb and ^{115}Mo are displayed in Fig. 2 with the identified transitions depopulating from the isomeric states. The exponential curves of isomeric decay obtained by applying the gates of delayed γ-rays, are fitted with the unbinned Maximum Likelihood Method to extract the half-lives. The reduced transition strength $B(\sigma\lambda)$ in ^{111}Zr, ^{113}Nb, ^{115}Mo are extracted by assuming different multipolarity (see Table. I) and taking into account the Internal Conversion coefficients calculated using BrIcc [32]. Excitation energies of the isomeric states in ^{111}Zr, ^{113}Nb, ^{115}Mo are much lower than the energy needed to break a pair of protons and neutrons($2\Delta_\pi =$ 2.5 MeV and $2\Delta_\nu = 2.1$ MeV [33, 34]), indicating their origins from single proton or neutron configurations.

III. RESULTS AND DISCUSSION

Because of the limited information in this measurements, the spins and parities of levels, as well as their associated collective structures, cannot be well investigated. However, some key characteristic properties of the gamma transitions could be identified and indicated.

The isomeric state decaying to the ground state via a transition of 265-keV was observed in ^{111}Zr, with an isomeric ratio estimated at 17 (2) %. The half-life was measured to be a value of 0.10(7) μs by fitting the decay curve in coincidence with the 265-keV transition (see Fig. 2 (top)). The calculated transition strengths when assuming various transition types (see Table. I) ruled out $M2$ and higher-multipole transitions due to their strengths exceed the recommended upper limit for each type of transition [35]. The small isomeric ratio indicates the higher spin of the isomeric state compared to the one of ground state since the high-spin excited states are favored to be populated by the in-flight fission and fragmentation mechanism [36–38],.

The isomeric state at 135-keV was first identified in ^{113}Nb, with a half-life estimated at 0.7(4) μs (see Fig. 2 (middle)). The isomeric ratio was determined to be 9(2)% by a ratio between the adopted level intensity and total implanted ^{113}Nb events. The $M2$ and higher-multipole transitions were ruled out due to their strengths exceed the recommended upper limit for each type of transition [35] (see Table. I). The small isomeric ratio suggests that the spin of isomeric state is larger than the one of ground state [36–38].

The isomeric state at 198 keV was first identified in ^{115}Mo, with an isomeric ratio and a half-life estimated at more than 90% and 46(3) μs (see Fig. 2 (bottom)). The proposed level scheme of ^{115}Mo with the tentatively assigned spins and parities are displayed in Fig. 3. The intensity of the 94-keV gamma line in the spectrum is divided and placed as a doublet, to account for the energy of the 188-keV level (see Fig. 2 (bottom)). The energy 10-keV transition between the 198-keV and 188-keV levels is too small to be observed with the current experimental setup. The relative intensities of transitions were displayed in Table. II. The large isomeric ratio indicates the lower spin of 198-keV level compared to the one of ground state [36–38].

IV. SUMMARY

In summary, the isomeric states in ^{111}Zr, ^{113}Nb, ^{115}Mo have been identified with the decent decay spectroscopy technique, which provide the first spectroscopy in the well-known nuclear region of prolate-to-oblate shape phase transition. Future researches are essential to study in detail about the shape transition in this region, by employing more direct experimental techniques, such as Coulomb Excitation, Charge Radius measurements etc.

TABLE I. γ-ray relative intensities and B($\sigma\lambda$) values for transitions depopulating the isomeric state in ^{111}Zr, ^{113}Nb, ^{115}Mo, assuming different multipolarity.

		$B(\sigma\lambda)$ (W.u.)				
Nuclei	Eγ (keV)	E1	M1	E2	M2	E3
^{111}Zr	265	$1.6^{+36}_{-7} \times 10^{-7}$	$1.2^{+27}_{-5} \times 10^{-5}$	$1.3^{+31}_{-5} \times 10^{-1}$	$1.0^{+22}_{-4} \times 10$	$1.6^{+37}_{-7} \times 10^{5}$
^{113}Nb	135	$1.6^{+21}_{-6} \times 10^{-7}$	$1.2^{+15}_{-5} \times 10^{-5}$	$4.0^{+53}_{-15} \times 10^{-1}$	$2.4^{+31}_{-9} \times 10$	$7.4^{+98}_{-27} \times 10^{5}$
^{115}Mo	198	$6.1^{+123}_{-24} \times 10^{-11}$	$4.7^{+95}_{-19} \times 10^{-9}$	$9.3^{+187}_{-37} \times 10^{-5}$	$7.2^{+143}_{-29} \times 10^{-3}$	$2.2^{+43}_{-9} \times 10^{2}$
	10	$4.4(4) \times 10^{-7}$	$1.6(1) \times 10^{-5}$	$2.8(2) \times 10^{-1}$	$2.8(2) \times 10$	$8.1(9) \times 10^{5}$

TABLE II. γ relative intensities observed in ^{115}Mo

Eγ (keV)	E$_i$ (keV)	E$_f$ (keV)	Relative Intensity
198	198	0	9(6)
188	188	0	100(6)
94	188	94	2(1)
94	94	0	2(1)

V. ACKNOWLEDGEMENT

This work was carried out at the RIBF operated by RIKEN Nishina Center and CNS, University of Tokyo. This research was sponsored in part by the Office of Nuclear Physics, U.S. Department of Energy under Awards No. DE-AC02-06CH11357 (ANL), No. DE-FG02-96ER40983 (UTK) and No. DE-AC05-00OR22725 (ORNL), and by the National Nuclear Security Administration under the Stewardship Science Academic Alliances program through DOE Award No. DE-NA0002132, by the National Science Foundation under Grants No. PHY-1430152 (JINA Center for the Evolution of the Elements), No. PHY-1565546 (NSCL), and No. PHY1714153 (Central Michigan University), by the Polish National Science Center under Contract No. UMO-2015/18/E/ST2/00217, by JSPS KAKENHI (Grants No. 14F04808, No. 17H06090, No. 25247045, and No. 19340074), by the UK Science and Technology Facilities Council ST/P005314/1, by NKFIH (NN128072), by the Janos Bolyai research fellowship of the Hungarian Academy of Sciences, by the UNKP-18-4-DE-449 New National Excellence Program of the Ministry of Human Capacities of Hungary, by Spanish Ministerio de Economia y Competitividad grants (FPA2017-83946-C2-1-P, FPA2011-28770-C03-03, FPA2014-52823-C2-1-P, FPA2014-52823-C2-2-P, FPA2014-57196-C5-4-P, FPA2017-84756-C4-2-P, SEV-2014-0398, and IJCI-2014-19172), by the Ministerio de Ciencia e Innovacion grant PID2019-104714GB-C21, by European Commission FP7/EURATOM Contract No. 605203, by the H2020 Euratom SANDA project (grant no. 847552), by the UK Nuclear Data Network funded by the UK Science and Technology Facilities Council Grant No. ST/N00244X/1, by the National Research Foundation (NRF) in South Korea (Grants No. 2016K1A3A7A09005575 and No. 2015H1A2A1030275), and by the Natural Sciences and Engineering Research Council of Canada (NSERC) via the Discovery Grants No. SAPIN-2014-00028 and No. RGPAS 462257-2014. Theoretical calculation in this letter was supported by the National Natural Science Foundation of China under Grants No. 11835001 and 12035001.

[1] M. Goeppert Mayer, Physics , 20 (1963).
[2] S. A. Johansson, Nucl. Phys. **64**, 147 (1965).
[3] T. Otsuka and Y. Tsunoda, J. Phys. G **43**, 024009 (2016).
[4] D. Arseniev, A. Sobiczewski, and V. Soloviev, Nucl. Phys. A **139**, 269 (1969).
[5] R. Sheline, I. Ragnarsson, and S. Nilsson, Phys. Lett. B **41**, 115 (1972).
[6] T. Sumikama et al., Phys. Rev. Lett. **106**, 202501 (2011).
[7] E. Cheifetz, R. C. Jared, S. G. Thompson, and J. B. Wilhelmy, Experimental information concerning deformation of neutron rich nuclei in the $a \sim 100$ region, Phys. Rev. Lett. **25**, 38 (1970).
[8] F. Browne et al., Phys. Lett. B **750**, 448 (2015).
[9] J. Ha et al., Phys. Rev. C **101**, 044311 (2020).
[10] F. R. Xu, P. M. Walker, and R. Wyss, Phys. Rev. C **65**, 021303 (2002).
[11] P. Mller, A. Sierk, T. Ichikawa, and H. Sagawa, At. Data Nucl. Data Tables **109-110**, 1 (2016).
[12] P. Kumar et al., Eur. Phys. J. A **36**, 2021 (2021).
[13] J. P. Delaroche, M. Girod, J. Libert, H. Goutte, S. Hilaire, S. Péru, N. Pillet, and G. F. Bertsch, Phys. Rev. C **81**, 014303 (2010).
[14] N. Paul et al., Phys. Rev. Lett. **118**, 032501 (2017).
[15] L. Geng, H. Toki, S. Sugimoto, and J. Meng, Prog. Theo. Phys. **110**, 921 (2003).
[16] B. Sorgunlu and P. Van Isacker, Nucl. Phys. A **808**, 27 (2008).
[17] K. L. Kratz et al., Eur. Phys. J. A **25**, 633 (2005).
[18] H. Watanabe et al., Phys. Lett. B **704**, 270 (2011).
[19] G. Lorusso et al., Phys. Rev. Lett. **114**, 192501 (2015).
[20] F. Montes et al., Astro. phys. J. **671**, 1685 (2007).

[21] N. Fukuda, T. Kubo, T. Ohnishi, N. Inabe, H. Takeda, D. Kameda, and H. Suzuki, Nucl. Inst. Meth. B **317**, 323 (2013).
[22] S. Nishimura et al., , RIKEN Accel. Prog. Rep. **46**, 182 (2013).
[23] R. Yokoyama et al., Nucl. Inst. and Meth. A **937**, 93 (2019).
[24] A. Tolosa-Delgado et al., Nucl. Inst. and Meth. A **925**, 133 (2019).
[25] A. Tarifeño-Saldivia et al., J. Inst. **12**, P04006 (2017).
[26] S. Nishimura, Prog. of Theo. and Exp. Phys. **2012**, 03C006 (2012).
[27] P.-A. Söderström et al., Nucl. Inst. Meth. B **317**, 649 (2013).
[28] J. Wu et al., , AIP Conf. Proc. **1594**, 388 (2014).
[29] J. Tain et al., Acta Phys. Pol. B **49**, 417 (2018).
[30] Z. Y. Xu et al., Phys. Rev. Lett. **113**, 032505 (2014).
[31] J. Wu et al., Phys. Rev. Lett. **118**, 072701 (2017).
[32] T. Kibdi, T. Burrows, M. Trzhaskovskaya, P. Davidson, and C. Nestor, Nucl. Inst. Meth. A **589**, 202 (2008).
[33] F. Kondev, M. Wang, W. Huang, S. Naimi, and G. Audi, The nubase2020 evaluation of nuclear physics properties *, Chinese Physics C **45**, 030001 (2021).
[34] P. Mller and J. Nix, Nucl. Phys. A **536**, 20 (1992).
[35] P. Endt, At. Data Nucl. Data Tables **26**, 47 (1981).
[36] J. Wilson et al., Nature **590**, 566 (2021).
[37] M. Bowry et al., Phys. Rev. C **88**, 024611 (2013).
[38] M. Bentaleb et al., Z. Phys. A **348**, 245 (1994).
[39] T. Togashi, Y. Tsunoda, T. Otsuka, and N. Shimizu, Phys. Rev. Lett. **117**, 172502 (2016).
[40] H. Watanabe et al., Phys. Lett. B **696**, 186 (2011).